Supplementary material

Detailed methods

Six African pygmy goats (*Capra hircus* L; 3 males, 3 females; mean ± standard deviation; age 21.0 ± 15.5 months, mass 25.85 ± 6.20 kg) were tested at Harvard University's Concord Field Station. EMG, fascicle, and tendon force data were recorded during a series of *in situ* and *in vivo* experiments. The experimental protocol involved four main steps over a three-day period: 1) surgical implantation of transducers, 2) *in vivo* testing, 3) surgical implantation of nerve cuffs, and 4) *in situ* testing. All experimental protocols have been described elsewhere (Lee et al., 2011, Wakeling et al., 2012, Lee et al. 2013).

Transducers

Offset twist-hook bipolar silver-wire electrodes (0.1 mm, California Fine Wire Inc., Grover Beach, CA) were implanted into the proximal, mid-belly, and distal portions of the lateral and medial gastrocnemius muscles.

Sonomicrometry crystals (2 mm, Sonometrics Inc., London, Ontario, Canada, resolution 0.3μm Lee et al., 2011), were implanted into the proximal, mid-belly, and distal regions of the lateral and medial gastrocnemius muscles in paired configuration such that the crystals were inserted parallel to the fascicles (proximo-superficial to distal-deep ~25° pennation angle), which allowed length changes of the fascicles to be estimated. The signal output was amplified (Triton 120.2; Triton Technology, San Diego, CA, USA) and monitored on an oscilloscope (2245A; Tektronix, Beaverton, OR, USA).

"E"-shaped stainless-steel buckle transducers, equipped with a metal foil strain gauge (type FLA-1, Tokyo Sokki Kenkyujo) bonded to the central arm (Biewener & Baudinette, 1995),

were attached to the Achilles tendon. On several goats, a 2 cm incision was made along the distal portion of the Achilles tendon and two separate tendon buckles were attached to the lateral and medial portions of the Achilles tendon, enabling separate recordings of LG and MG force.

In vivo *testing*

Goats were allowed 20-24 hrs for recovery following surgery. The animals had been previously trained to walk, trot, and gallop on a large, motorized treadmill (belt, 2.50 m long and 0.75 m wide) on a level surface. As part of a larger study, these gaits were performed on a level and incline surface (Lee et al., 2013); however, the models presented here are validated against the level gait conditions only. Recordings were collected at typical walking and running speeds such that five trials of at least 15-20 strides each were collected for each condition. Sufficient rest was given to the goats between trials to ensure that they could complete the experiments. Myoelectric signals were amplified (gain of 100-1000) and recorded with minimal filtering (bandpass 30-3000 Hz, notch filtered at 60 Hz, P511 amplifier, Grass, West Warwick, USA). Tendon buckle signals were connected to a bridge amplifier (Vishay 2120, Micro-Measurements, Raleigh, NC). All signals were recorded at 5000 Hz using a 16-channel acquisition device (NI-6259, National Instruments, Austin, TX). In addition, data were collected during tendon taps to the Achilles tendon to elicit action potentials from the slow motor units.

In situ *experiments – Nerve stimulation*

Prior to *in situ* testing, a secondary surgery took place where two tripolar nerve cuff were placed around the lateral and medial portion of the tibial nerve innervating the muscles. An additional force transducer was surgically attached on the medial portion of the Achilles tendon.

Animals were maintained on 0.5 – 1.0 % isoflurance anesthesia throughout the duration of the *in situ* experiments. The left hindlimb of each animal was secured in a customized stereotactic frame (80/20 Inc., Columbia City, IN) while the animal was placed on its side. The tibial nerve was stimulated under direct computer control (Labview 7.1, National Instruments Corp., Austin, TX; World Precision Instruments, Sarasota, FL). The ankle flexion-extension angle was adjusted in the frame and then fixed for each isometric contraction. The active and passive force-length relationship was measured using tetanic stimulation (at 40 Hz stimulation frequency) at each position. The ankle position corresponding to maximum tetanic force was identified so that subsequent contractions would be measured at the optimal muscle length. With the ankle secured at this position, each muscle was subjected to stimulation to elicit action potentials from either slow motor units or both slow and fast motor units. The force profiles of the twitch trials were used to derive the transfer functions which are described later.

Analysis of force data

Tendon forces were filtered using a low-pass third-order Butterworth filter with a cut-off frequency of 45 Hz and notch filter at 60 Hz. Calibration yielded r^2 values of 0.99. Tendon forces were normalized by the maximum force recorded during incline trotting, F_{max}, consistent with previous analyses (Lee et al., 2013). For the *in vivo* forces, lateral and medial tendon forces were estimated from the total tendon force using the ratio of the maximum forces measured from the *in situ* recordings of the lateral and medial gastrocnemius muscles from the two tendon buckles.

Analysis of sonomicrometric data

Sonomicrometry signals were converted to a distance measurement between the crystals based on the speed of sound through skeletal muscles, adjusted by a + 0.82 mm correction due to differences between the speed of sound through the epoxy coating of the crystals and the speed of sound through muscle (resolution = 0.3μm, Daley and Biewener, 2003). Sonomicrometry signals were first filtered using a low-pass, third-order Butterworth filter with a cut-off frequency of 45 Hz. A custom-written program was used to identify and remove "extraneous" peaks, after which the signals were fit with a moving 4^{th} order polynomial using a 200-point (40 ms) size window. Fascicle lengths were normalized to passive fascicle length (distance measured between the crystals during the *in situ* experiments that resulted in the maximum isometric force). Fascicle shortening rate was calculated as the first derivative of fascicle with respect to time.

Analysis of electromyography data

EMG signals from the *in vivo* measurements from the lateral and medial gastrocnemius muscles measured were analyzed using wavelet transformation, similar to previously published wavelet techniques (von Tscharner, 2000; Wakeling and Syme, 2002; Hodson-Tole and Wakeling, 2009; Lee et al., 2011; Lee et al., 2013). Briefly, the EMG signals were resolved into their intensities in time-frequency space using a filter bank of 19 non-linearly scaled wavelets with a total bandwidth of 101-1857 Hz (Lee et al., 2011). Using principal component analysis (PCA), the major features of the intensity spectra were identified so that a set of optimized wavelets could be calculated which represented the low and high frequency bands of the slow and fast motor units (Wakeling, 2005; Hodson-Tole and Wakeling, 2008; Lee et al., 2011). The

majority of the signal for any given myelectric spectrum was defined by the first two principal components: the relative PCI and PCII loading scores gave a measure of the frequency of the myoelectric signal. Two extreme spectra were identified from the first and second PCs that have been previously shown to correspond to the slower and faster motor units (von Tscharner and Goepfert, 2006; Wakeling and Horn, 2009; Lee et al., 2011). Subsequently, two new wavelets optimized to these spectra were derived. These optimized wavelets with specific center frequencies and bandwidth to slow and fast motor units allowed the intensities of the low and high frequency bands to be calculated.

Time resolution

In general, for this wavelet analysis method (von Tscharner, 2000), the time resolution varied for each wavelet. The optimized wavelets could have even shorter time-resolutions of 1.5 to 3 ms (Lee et al., 2011). In order to compare methods that have excitations derived from either the bank of wavelets or the optimized wavelets, it was necessary to set the time resolutions to be the same. The wavelet analysis had a final Gauss filter step to remove oscillations in the calculated intensity that were in fact artifacts of the method. For the purpose of this study, this Gauss filter step was kept the same for every wavelet so they had identical time resolutions. Wavelets with a 75 ms time resolution were found to best estimate activation by testing four different time resolutions (25, 50, 75, and 100 ms) to test the sensitivity of the method to this parameter. These time resolutions were within the range of physiological response time of muscle 10 ms and 100 ms (Levin et al., 1999; Spaegele et al., 1999).

Muscle contractile parameters

Activation

We assumed that the activation dynamics could be represented by a series of coupled first-order bilinear differential equations (similar to Zajac, 1989). Using the EMG intensity of the slow and fast motor units which were calculated with the optimized wavelets, and the reconstructed twitch force traces, we identified the values for the $\tau_{act\ 1,2,3}$, time constants, and $\beta_{1,2,3}$, constants which were related to the activation and deactivation time constants for the whole muscle as well as for the slower and faster motor units (Eq. SM1, Table 1, Lee et al., 2011). These constants were calculated by least squares minimization of the activation equation to the force-time curves for: 1) the total EMG intensity of the supramaximal twitches, 2) the high frequency component, and 3) the low frequency component of the EMG intensity of the supramaximal twitches obtained from the optimized wavelets. These transfer functions also incorporated a timing offset, t_{off}, which accommodated the electromechanical delay, and considered the different activation and deactivation rates and rise in activation that persists after the action potentials in the myoelectric signal dissipate to zero. Thus, using the derived transfer function, we calculated the activation state of the slow and fast motor fibers. These transfer functions were validated by correlating the predicted activation states with the measured force during the isometric contractions *in situ* (r^2=0.96 - 0.99). Activation was normalized to the maximum activation calculated during incline trotting. The activation levels of the slower and faster motor units were scaled in amplitude such that the summation of the two activation levels were equal to the amplitude of active state of the whole muscle (total activation).

$$\frac{d}{dt}(a_1) + \left[\frac{1}{\tau_{act1}}\left(\beta_1 + [1-\beta_1]EMG(t-t_{off})\right)\right]a_1(t) = \left(\frac{1}{\tau_{act1}}\right)EMG(t-t_{off})$$

$$\frac{d}{dt}(a_2) + \left[\frac{1}{\tau_{act2}}\left(\beta_2 + \left[1-\beta_2\right]a_1(t)\right)\right]a_2(t) = \left(\frac{1}{\tau_{act2}}\right)a_1(t) \quad \text{(Eq.SM1)}$$

$$\frac{d}{dt}(a_3) + \left[\frac{1}{\tau_{act3}}\left(\beta_3 + [1-\beta_3]a_2(t)\right)\right]a_3(t) = \left(\frac{1}{\tau_{act3}}\right)a_2(t)$$

Force-length

The force-length relation was determined for these goats as a function of fascicle length. The resting fascicle length was defined as the passive fascicle length at the ankle angle that yielded the maximum tendon force. Force-length properties, $\hat{F}(l)$, were normalized by the maximum active force. The active (Eq. SM2) and passive (Eq. SM3) force-length curves were based on *in situ* measurements, taken during supramaximal stimulation, at a range of fascicle lengths. These equations were derived by fitting the *in situ* data pooled from all six goats.

$$\hat{F}_{\mathrm{a}}(l) = \frac{((-878.25(l*1.253)^2 + 2200.4(l*1.254) - 1192)}{186.24} \quad \text{(Eq. SM2)}$$

$$\hat{F}_{\mathrm{p}}(l) = \frac{e^{-1.3+3.8*(l*1.253)}}{186.24} \quad \text{(Eq.SM3)}$$

Force-velocity

Maximum unloaded shortening velocities, v_o, (l_{opt} s^{-1}), were estimated for the slow- and fast- fibers using two methods. First, from a literature survey of 59 species from 88 papers, the following relation for locomotor muscles in terrestrial species was used (coefficient of determination, r^2 = 0.75; Wakeling et al., 2012; Hodson-Tole and Wakeling, personal communication):

$$v_0 = 71.1\tau_a^{-0.74} \quad \text{(Eq. SM4)}$$

where τ_a is the time to maximum twitch force (ms) and was estimated to be 98.6 and 52.9 ms for the slow and fast fibers, respectively (Lee et al., 2011) which gives v_0 values of 2.74 l_{opt} s^{-1} and 3.59 l_{opt} s^{-1} for the slow and fast fibers, respectively. To test the sensitivity of the muscle force prediction to the values of v_0, we chose two values based on ranges of v_0 reported in the literature for the mouse, rat, and cat at physiological temperature, 4.8 to 7.3 l_{opt} s^{-1} for slow fibers and 9.2 and 24.2 l_{opt} s^{-1} for fast fibers. No values are reported for large mammals so adjusting for size, as large animals have lower v_0 , we selected values of 5 and 10 3 l_{opt} s^{-1} for v_0 for the slow and fast fibers, respectively (Wakeling et al., 2012).

Muscle Models

Four muscle models were used to estimate muscle force F_m (see summary of parameters in Table 3). The total muscle force was estimated by:

$$F_m = c\left[\hat{F}_f + \hat{F}_p(l)\right]\cos\theta \quad \text{(Eq. SM5)}$$

where $\hat{F}_f$ is the active component of the muscle fiber force and $\hat{F}_p$ is the passive component of the force as a function of fiber length (l). Constant c and the pennation angle, θ, scaled the fiber force to the whole muscle force. In particular, constant c scaled the predicted force from its normalized value to the measured force for each goat. Thus, c reflects the maximum isometric force generated by the muscle. The pennation angle was calculated at each time step as a function of fiber length (l) from the resting pennation angle and the fascicle length, assuming that the thickness of the muscle remained constant (Zajac, 1989; Millard and Delp, 2012; van den Bogert et al., 2011). For three models (homogenous, hybrid, orderly), the active component of the muscle fiber force was given by:

$$\widehat{F_f} = \hat{a}(t)\widehat{F_a}(l)\widehat{F_v}(v) \quad \text{(Eq. SM6)}$$

where $\hat{a}(t)$ is the time-varying activation level (Lee et al., 2011) normalized to the maximum activation measured during the *in vivo* experiments (Lee et al., 2013), and $\hat{F}_{\mathrm{a}}(l)$ is the active force-length relationship normalized to a maximum of 1.

The force-velocity relationship, $\hat{F}_{\mathrm{v}}(v)$, was given by:

$$\hat{F}_{\mathrm{v}}(v) = \frac{\left(1 - \frac{v}{v_o}\right)}{\left(1 + \frac{v}{v_o k}\right)} \text{ for } v \leq 0 \quad \text{(Eq. SM7)}$$

$$\hat{F}_{\mathrm{v}}(v) = 1.5 - 0.5\frac{\left(1 + \frac{v}{v_0}\right)}{\left(1 - \frac{7.56v}{v_{\mathrm{o}}k}\right)} \text{ for } > 0 \quad \text{(Eq. SM8)}$$

where v is the fiber contractile velocity, v_0 is the maximum intrinsic speed, and constant k characterizes the curvature of the force-velocity curve and varies according to muscle fiber type. Note that shortening velocity is defined as negative in these equations, while lengthening is defined as positive. In a literature survey of 59 species from 88 papers (Wakeling et al., 2011; Hodson-Tole and Wakeling, personal communication), the curvature for the faster fibers of muscle used primarily for locomotion was reported to be flatter than that of slower fibers (k = 0.29 and k = 0.18, respectively). Different values of v_0 and k were assigned for the different models, based on assumptions about motor unit recruitment, as described in the following sections.

The **homogenous model** assumed that the muscle consisted of fibers with homogenous properties. v_0 was the maximum intrinsic speed of the different fiber types weighted by their fractional cross-sectional area. The curvature k was assigned an intermediate value between the slow and fast fibers range and was assumed to be the same all the fibers within the muscle.

$$k = k_{slow} + (k_{fast} - k_{slow})p \quad \text{(Eq. SM9)}$$

where p is the fractional area of the fast fibers. Since p is presently unknown for goat, values of 0.75 and 0.5 were used to incorporate the range of slow and fast fiber proportions in the gastrocnemius muscles. From immunohistochemical testing, the LG contained a higher proportion of fast fibers in goat muscles (unpublished observations, Carr, Miara, Lee, Wakeling, and Biewener).

The **hybrid model** was the same as the homogenous model except that v_0 represented the fastest fibers and k was calculated from the combination of the force-velocity relation of slow and fast fibers with forces proportional to their fractional fiber area (Hill, 1970). This value of k was greater than that calculated using Eq. SM9.

The **orderly recruitment model** assumed that the active muscles display intrinsic properties of progressively faster fiber types as activation levels increase. Thus, at initial low activation levels, the active fibers had slow fiber intrinsic properties. This model was based on classical studies of orderly recruitment during steady stretch reflexes (Hennemen, 1974) and followed previous muscle models approaches (Umberger et al., 2000; Van Soest et al., 1993).

$$v_0 = v_{0,slow} + (v_{0,fast} - v_{0,slow})\,\hat{a}(t) \quad \text{(Eq. SM10)}$$

The **differential recruitment model** (Figure 1) incorporated independently activated slow and fast contractile elements in parallel (Wakeling et al., 2012). The EMG intensity at the low- and high- frequency bands, determined from the EMG and optimized wavelets, were used with the transfer functions (Eq. SM1 and Table 1) to estimate the activation levels for the slow and fast elements, $\hat{a}_{slow}(t)$ and $\hat{a}_{fast}(t)$, respectively. The total muscle active force from the fibers

was given by:

$$\hat{F}_{\mathrm{f}} = \hat{F}_{\mathrm{f,slow}} + \hat{F}_{\mathrm{f,fast}} \qquad \text{(Eq. SM11)}$$

where $\hat{F}_{\mathrm{f,slow}}$ and $\hat{F}_{\mathrm{f,fast}}$ are the normalized forces for slow and fast fibers, respectively, as determined from Eq. SM4 using fiber-specific values of $\hat{a}(t)$, v_0 , and k (Tables SM1 and 3).

Results

The two-element muscle model generally performed better than the one-element models. In particular, the differential model predicted time-varying LG forces with significantly higher r^2 (better correlation) and lower RMSE (less error) than the one-element models, both during galloping (r^2, $p < 0.04$; RMSE, $p < 0.001$; Figs. SM1 and SM2) and during trotting (RMSE, $p < 0.001$). The differential model also predicted time-varying MG forces with significantly lower RMSE than the one-element models during trotting and galloping ($p < 0.001$ and $p < 0.01$, Fig. 4). The r^2 and RMSE values of the three one-element muscle models were not significantly different from one another across all gaits.

Discussion

Limitations

One of the aims of this study was to examine the ability of current and commonly used Hill-type models to accurately reproduce muscle forces measured *in vivo*. Despite the improvements achieved by incorporating slow and fast contractile elements into Hill-type models, all of models evaluated in this study have limitations that may have contributed to the errors in magnitude and timing. For example, the muscle models that we examined all assume

that activation, force-length, and force-velocity properties are independent, though it has been shown that activation is influenced by muscle length (Balnave et al., 1996; Close et al., 1972; Stephenson et al., 1984). Activation also strongly influences length-tension and force-velocity behavior (Joyce et al., 1994; Brown et al., 1999; Sandercock and Heckman, 2001). Finally, none of these models explicitly account for history-dependent effects and fatigue, which are known to affect muscle force generation (Rassier et al., 2003; Edwards, 1981). Since faster fibers fatigue more rapidly than slower fibers (Burke et al., 1973), and since the two-element model accounts for time-varying changes in activation of the different motor units, it is possible that the two-element model is more robust to fatigue than the one-element models tested.

In many of the simulations, we observed errors in relative phasing between predicted and measured force in which modeled forces developed earlier than *in vivo* force. The time resolution of the Gauss filter applied in the wavelet analysis may have contributed to errors in the relative phasing between predicted and measured force. The time resolution of the filter affected the accuracy of force prediction because our estimates of EMG intensity for the whole muscle were based on recordings of fine-wire EMG from a small population of motor units. The time resolution we ultimately selected (75 ms) was chosen based on a rigorous sensitivity analysis (see supplementary material for more detail) and is within the physiological range of the response time of muscle (10 ms and 100 ms; Levin et al., 1999; Spaegele et al., 1999). The time resolution of the wavelet analysis (75 ms) was longer than the time resolution of the original EMG analysis (20 ms; von Tscharner, 2000) and was longer than the time resolution of the optimized wavelets (1.5 ms; Lee et al. 2011). The longer time resolution was used because it smoothed rapid fluctuations in the EMG signal, which are an inevitable consequence of recording from a limited number of motor units. A result of this smoothing is that the EMG

intensities appear sooner and persist longer than the raw signal; this may explain the early rise in the predicted forces evident in Figure. 2. The persistence of EMG intensity after decay of the raw signal is less likely to affect the predicted forces because the transfer function to calculate activation state (Eq. 1) has a longer time constant for deactivation and predicts activation long after the EMG signal has diminished (Lee et al. 2011). If surface EMG rather than fine-wire EMG was used to estimate activation state (which is common when studying human subjects), then a larger population of motor units could be sampled and the time-resolution of the analysis reduced, thereby improving the timing of the predicted force.

Errors in the phasing between the predicted and measured forces may also have resulted, in part, from not including a tendon in the muscle models. Force was measured from a buckle transducer on the Achilles tendon, and timing delays that may have been introduced, relative to the muscle's force profile, would not have been captured by our models. We considered including an elastic component and damping in the models, but elected to take a simpler approach so that model parameters could be based on experimental measures, in which we have confidence.

Validation

We previously evaluated the accuracy of MG and LG forces predicted by our two-element model during *in situ* experiments (Wakeling et al., 2012). The comparisons with *in situ* forces yielded higher r^2 values (0.8 to 0.95) than the comparisons with *in vivo* forces reported here. This difference is not necessarily surprising, since the *in situ* conditions were more controlled than those observed *in vivo* (Wakeling et al., 2012). To gain more insight into the model's performance during *in situ* and *in vivo* experiments, we examined the percentage

difference in r^2 values between the forces predicted by the one-element and two-element models. Under *in situ* conditions, the r^2 value was up to 9.7% higher for the two-element model than for the one-element models tested. Under *in vivo* conditions, the r^2 value was up to 37.4% higher and the RMSE was as much as 32.2% lower for the two-element model than for the one-element models. Thus, the two-element model predicted force more accurately than the one-element model under *in situ* and *in vivo* conditions (Figures 3-4).

Very few studies have validated Hill-type models under functionally relevant conditions. Many studies have evaluated models based on *in situ* data, but these tests have generally been performed under laboratory conditions where fascicle lengths and activations are not typical of those observed *in vivo*. When large changes in muscle length have been imposed *in situ,* %RMSE errors have been reported to exceed 50% (Perreault et al., 2003). Some previous studies have reported smaller errors (~10%), but only under controlled *in situ* conditions with tetanic or near-tetanic stimulation up to 30% of maximum isometric force (van Ingen Schenau et al., 1988; Sandercock and Heckman, 1997). A strength of the current study is that inputs driving the models, along with most parameters, were based on experimental measures from the same set of muscles from which force was measured *in vivo*. Thus, the errors reported here for *in vivo* locomotor tasks are especially informative – revealing the strengths and weaknesses of Hill-type models under physiologically relevant conditions.

Table SM1. Force-velocity properties and activation state for the one- and two-element models.

Model	Force-velocity curvature, k	Maximum unloaded shortening velocity, v_0	Activation state
Homogenous	$k_{slow} + (k_{fast} - k_{slow})p$	$v_{o,fast}\,p + v_{o,slow}\,(1 - p)$	$\hat{a}(t)$
Hybrid	Composite from Hill (1970)	$v_{o,fast}$	$\hat{a}(t)$
Orderly	$k_{slow} + (k_{fast} - k_{slow})p$	$v_{o,slow} + (v_{o,fast} - v_{o,slow})\ \hat{a}(t)$	$\hat{a}(t)$
Differential	k_{slow}	$v_{o,slow}$	$\hat{a}_{slow}(t)$
	k_{fast}	$v_{o,fast}$	$\hat{a}_{fast}(t)$

1

Figure SM1. Coefficient of determination between the measured and predicted forces for the different muscle models, as determined for the different gait conditions and for the a) LG and b) MG muscles. Bars show the mean ± SEM pooled from all the goats. Models were assigned v_o values of 5 and 10 $l_{opt}s^{-1}$ for the slow and fast fibers, respectively, with a fiber-type proportion of 75% fast fibers. *Post hoc* Tukey tests were conducted to identify significant differences between the models for each gait, and these differences are denoted by the horizontal bars.

Figure SM2. Root mean square error (RMSE) in the predicted forces, as a percentage of the maximum measured *in vivo* force, for the different muscle models, as determined for the different gait conditions and for the a) LG and b) MG muscles. Bars show the mean ± SEM pooled from all the goats. Models were assigned v_o values of 5 and 10 $l_{opt}s^{-1}$ for the slow and fast fibers, respectively, with a fiber-type proportion of 75% fast fibers. *Post hoc* Tukey tests were conducted to identify significant differences between the models for each gait, and these differences are denoted by the horizontal bars.

Figure SM1

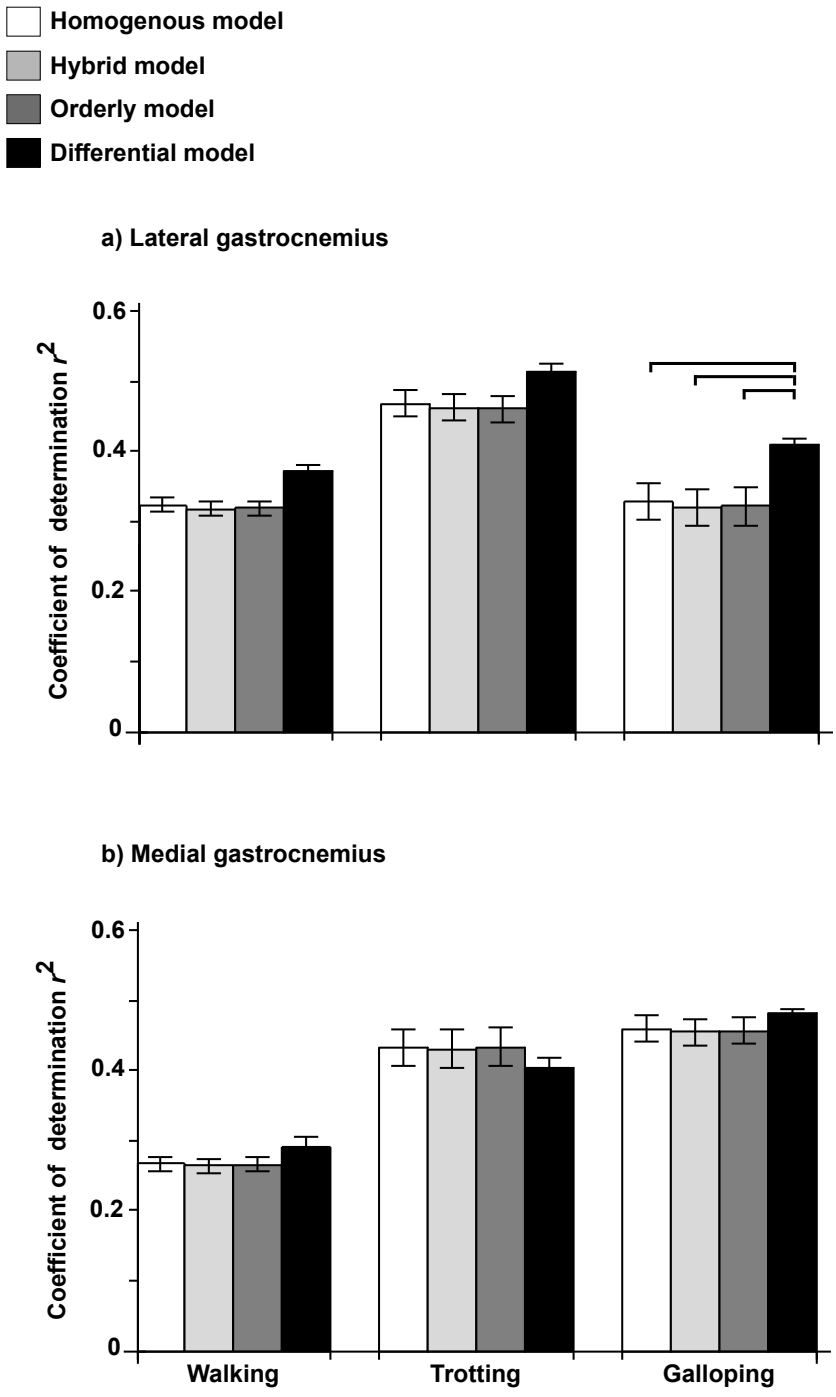
Homogenous model
Hybrid model
Orderly model
Differential model
a) Lateral gastrocnemius
Coefficient of determination r^2
0.6
0.4
0.2
0
b) Medial gastrocnemius
Coefficient of determination r^2
0.6
0.4
0.2
0
Walking
Trotting
Galloping

Figure SM2

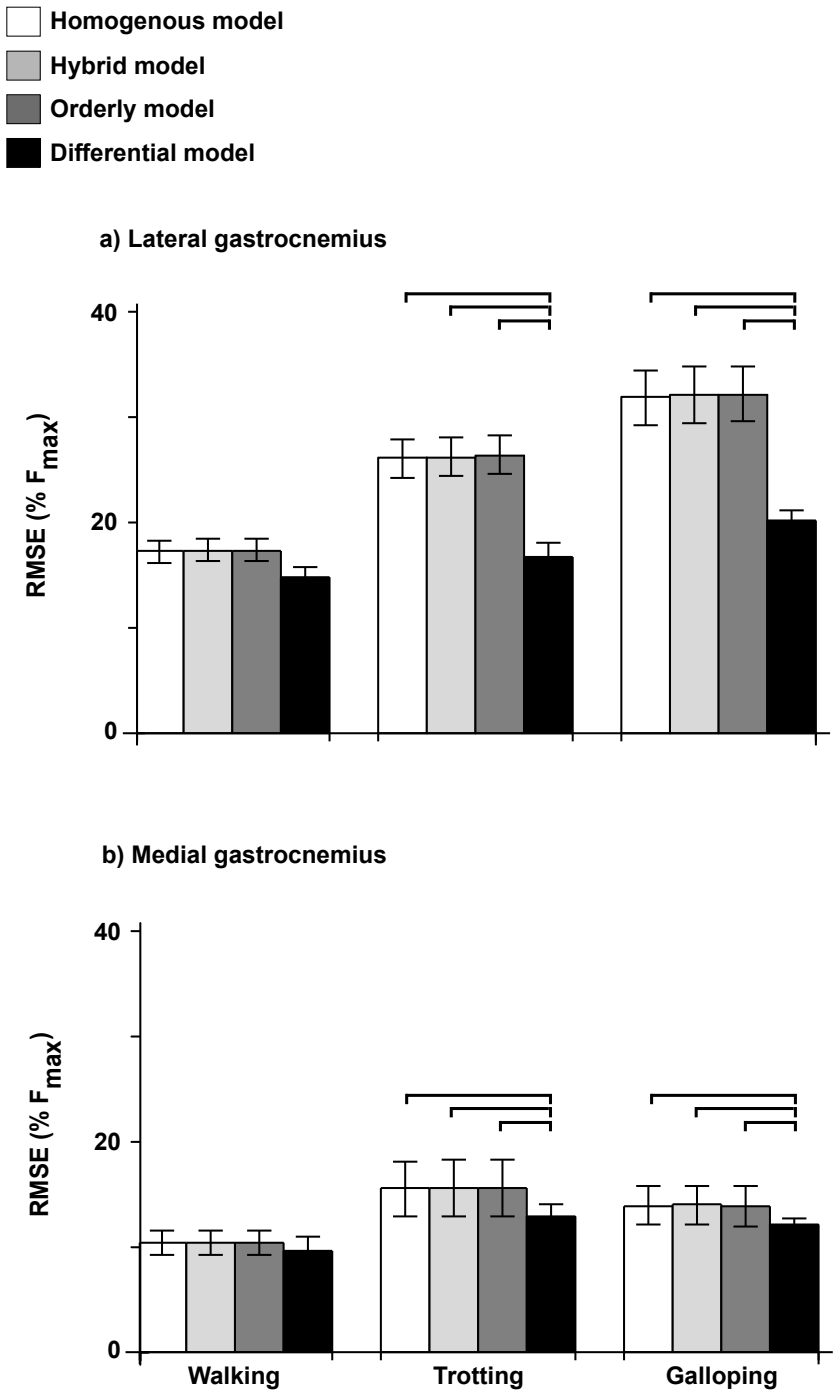
Homogenous model
Hybrid model
Orderly model
Differential model
a) Lateral gastrocnemius
RMSE (% F max)
40
20
0
b) Medial gastrocnemius
RMSE (% F max)
40
20
0
Walking
Trotting
Galloping